Supporting Information

Wireless, Flexible, and Disposable Sensing Devices Enabling Real-time Long-term Patient Medical Care for Pressure Injury Prevention

Ta Sheng-Chang,[1] Chiao-Wen Chien,[1] Elmer Ismael Guerra,[1] Ting-Yi Wang,[1] Chien-Wei Huang,[1] Ying-Siou Lin,[3,4] Jung-Chen Chang,[3,4]* and Wei-Ssu Liao[1,2]**

[1] Department of Chemistry, National Taiwan University, Taipei 10617, Taiwan

[2] Center for Emerging Material and Advanced Devices, National Taiwan University, Taipei 10617, Taiwan

[3] School of Nursing, College of Medicine, National Taiwan University, Taipei 10051, Taiwan

[4] Department of Nursing, National Taiwan University Hospital, Taipei 100229, Taiwan

*To whom correspondence should be addressed: yingsiou0217@ntuh.gov.tw (Ying-Siou Lin); jungchenchang@ntu.edu.tw (Jung-Chen Chang); wsliaochem@ntu.edu.tw (Wei-Ssu Liao)

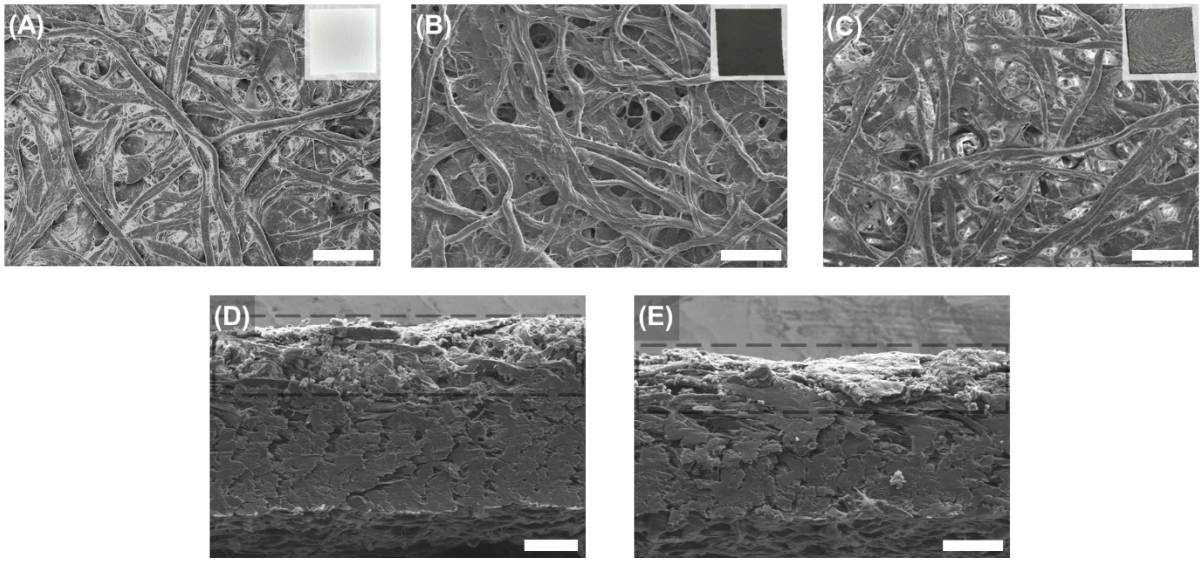

Figure S1. SEM images of (A) pristine filter paper, (B) CNT-coated paper obverse and (C) reverse side, and cross-section images of filter paper decorated with (D) 3:7 and (E) 4:6 ratio of CNT:PEDOT solution. The marked region in (D) and (E) represents the penetration area of composites. The scale bar is 100 μm. The insets are photos of sample filter papers with 2 cm in length.

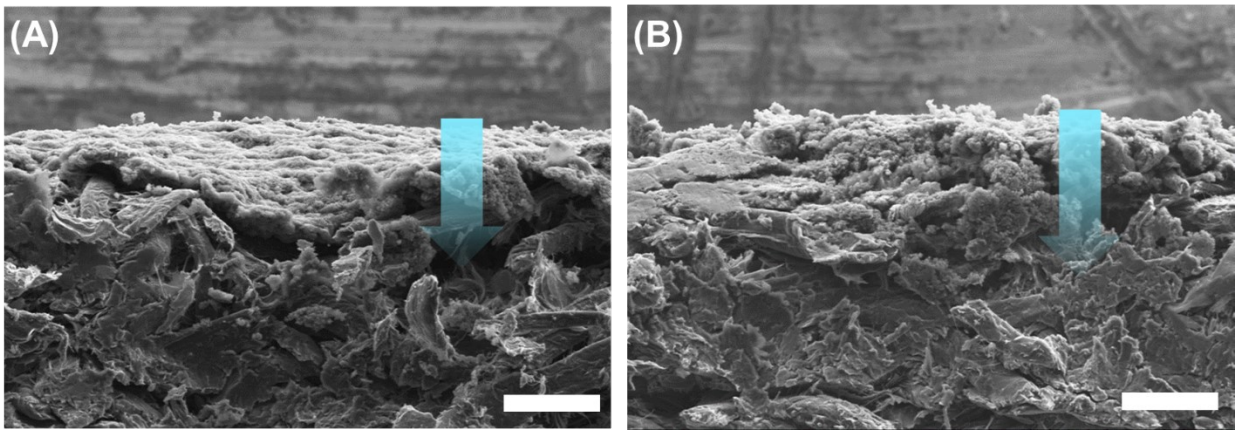

Figure S2. SEM cross section images of the obverse (A) and reverse (B) side of CNT-PEDOT composite/paper utilizing 3:7 CNT:PEDOT ratio prepared by the double-side dropping method. The scale bar is 100 μm.

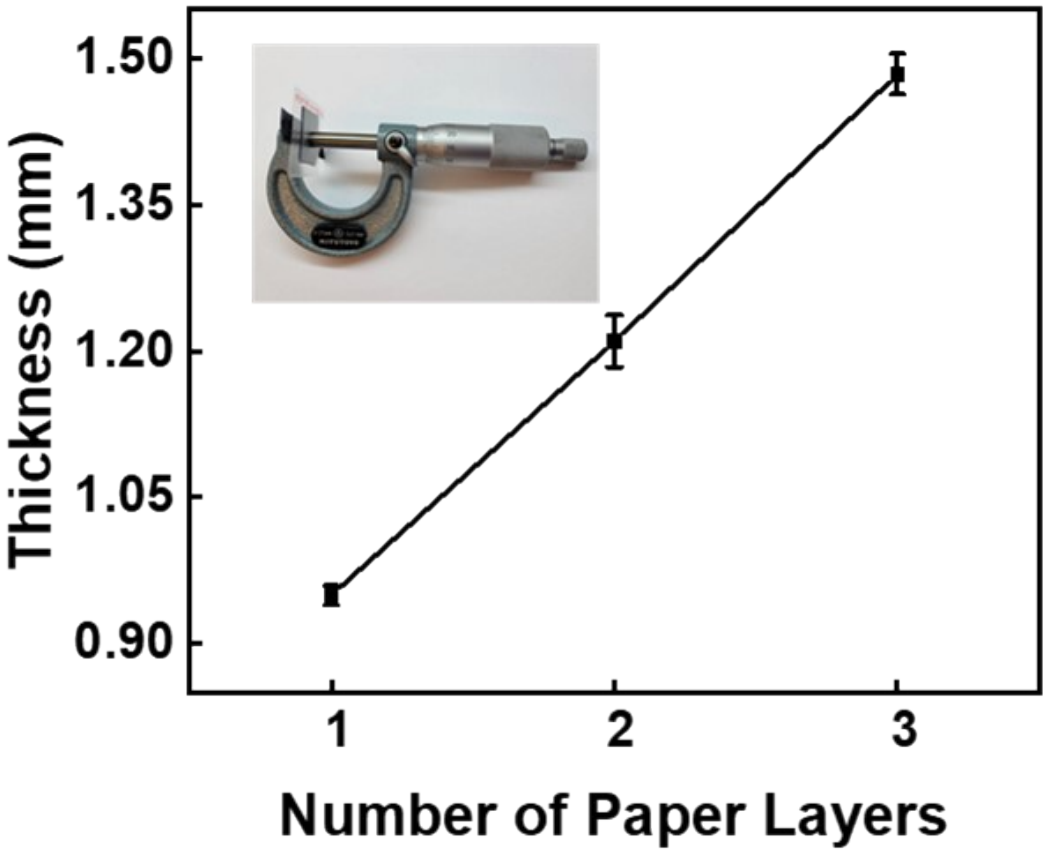

Figure S3. Thickness of the integrated sensor combining different numbers of paper layers. The inset presents the measuring method.

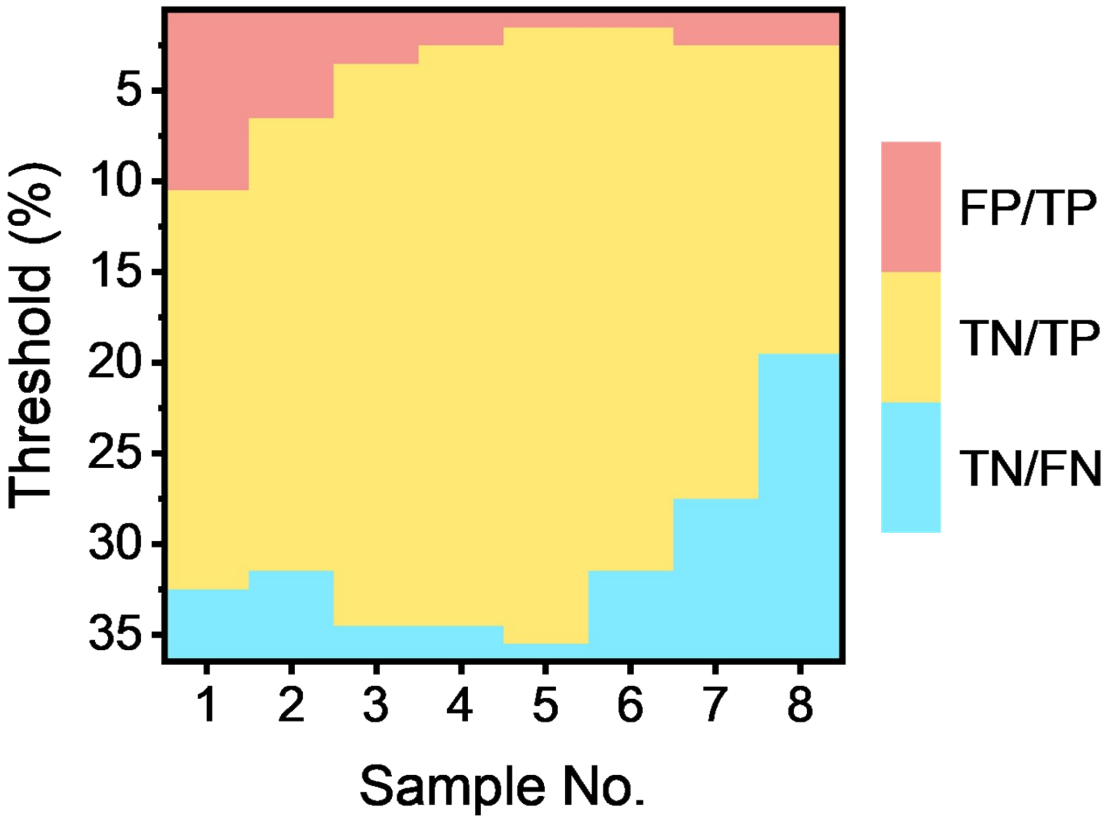

Figure S4. The heat map of error types for multiple devices with different thresholds ($N = 8$).

Table S1. Comparison of representative conventional pressure sensors applied in human motion detection.

Material	Mechanism	Application	Sensitivity (Sensing Range)	Ref. No.
Graphite Filler in Silicone Rubber on Paper Substrate	Conductance Distance Change	Finger Motion, Speech Detection	~40 kPa^{-1} (0 – 12 kPa)	1
PEI-CNT Deposited on Wool Fibers	Fiber–Fiber Electrical Contacts	Finger Touching, Weighting	~0.05 MPa^{-1} (0 – 40 MPa)	2
ZnOEP/CNT Hybrid on PDMS Micropost Array	Cobweb-like Network Compression	Wrist Pulse, Speech Detection	39.4 kPa^{-1}, (0 – 1.6 kPa)	3
Dip-coated Plastic Textile with Polymer-CNT	Fabric Contacts from Conductive Pathway	Human Motion, Respiration, Elbow and Wrist Bending	147.1 kPa^{-1}, (0 – 50 kPa)	4
Dip-coated Textile with MXene	Shape Deformation of MXene–textile	Finger Touching, Wrist Pulse, Sensing Array	3.844 kPa^{-1} (< 29 kPa)	5
Ag Wrinkles Coated on PDMS	Wrinkle Deformation and Vibration	External Sound Sensing	~2 kPa^{-1} (1 – 6 kPa)	6

The Evaluation of Signal Distinction Validity with Paired t-test

The Paired *t*-test is applied to compare the compressed and uncompressed states of the sensors, as the pairs of measurements are used to minimize sources of variability. The null hypothesis is set as $\mu_d = \Delta_0 = 0$, and the alternative hypothesis is $\mu_d \neq 0$. The paired *t*-test is conducted with the formula

$$t = \frac{(d - \Delta_0)}{s/\sqrt{N}}$$

where d is the averaged $\Delta R/R_0$ difference between the two states. The standard deviation (s) from the mean $\Delta R/R_0$ difference is adopted. The variation of two states for each sample is presented in Table S1. From the results, the average difference d is determined as 28.02%, with a standard deviation of 4.771%. ($N = 7$) The t value is calculated as 15.54, which surpasses the critical value of t as 5.41 for the 99% confidence level. Thus, the null hypothesis is rejected, concluding that the pressure sensors present different relative resistance changes under the compressed and uncompressed states.

Table S2. The $\Delta R/R_0$ differences between compressed and uncompressed states of the sensors.

Sample No.	**1**	**2**	**3**	**4**	**5**	**6**	**7**
Differences (%)	29.72	24.25	23.70	21.92	30.24	31.53	34.82

REFERENCES

1. Lin, X. Z.; Gao, S.; Fei, T.; Liu, S.; Zhao, H. R.; Zhang, T. Study on a Paper-Based Piezoresistive Sensor Applied to Monitoring Human Physiological Signals. *Sens. Actuators, A* **2019,** *292*, 66-70.

2. Doshi, S. M.; Thostenson, E. T. Thin and Flexible Carbon Nanotube-Based Pressure Sensors with Ultrawide Sensing Range. *ACS Sens.* **2018,** *3*, 1276-1282.

3. Zhang, W.; Xiao, Y.; Duan, Y.; Li, N.; Wu, L.; Lou, Y.; Wang, H.; Peng, Z. A High-Performance Flexible Pressure Sensor Realized by Overhanging Cobweb-like Structure on a Micropost Array. *ACS Appl. Mater. Interfaces* **2020,** *12*, 48938-48947.

4. Zhang, L.; He, J.; Liao, Y.; Zeng, X.; Qiu, N.; Liang, Y.; Xiao, P.; Chen, T. A Self-Protective, Reproducible Textile Sensor with High Performance towards Human–Machine Interactions. *J. Mater. Chem. A* **2019,** *7*, 26631-26640.

5. Li, T.; Chen, L.; Yang, X.; Chen, X.; Zhang, Z.; Zhao, T.; Li, X.; Zhang, J. A Flexible Pressure Sensor Based on an MXene–Textile Network Structure. *J. Mater. Chem. C* **2019,** *7*, 1022-1027.

6. Li, Y.; Zhang, W.; Zhao, C.; Li, W.; Dong, E.; Xu, M.; Huang, H.; Yang, Y.; Li, L.; Zheng, L.; Mao, M.; Yao, S.; Wang, L.; Ma, J.; Wang, X.; Huang, W. Breaking the Saturation of Sensitivity for Ultrawide Range Flexible Pressure Sensors by Soft-Strain Effect. *Adv. Mater.* **2024,** *36*, 2405405.